Low-loss curved waveguide grating wavelength demultiplexer

Abdelfettah Hadij-ElHouati,[1,2,*] *Alejandro* Ortega-Moñux,[1,2] *J. Gonzalo* Wangüemert-Pérez,[1,2] *Robert* Halir,[1,2] *Shurui* Wang ,[3] *Jens* H. Schmid,[3] *Pavel* Cheben,[3] and *Iñigo* Molina-Fernández[1,2]

[1] Dept. de Ingeniería de Comunicaciones, ETSI Telecomunicación, Universidad de Málaga, Campus de Teatinos s/n, 29071 Málaga, Spain
[2] Instituto de Telecomunicación (TELMA), Universidad de Málaga, CEI Andalucía TECH, E.T.S. Ingeniería de Telecomunicación, Bulevar Louis Pasteur 35, 29010 Málaga, Spain
[3] National Research Council of Canada, Ottawa, Ontario, K1A 0R6, Canada

Abstract. We demonstrate a compact wavelength demultiplexer for the silicon on insulator platform based on the curved waveguide grating (CWG) architecture. We mitigate off-chip radiation loss by enforcing the single beam condition by using metamaterial index engineering. The fabricated device exhibits insertion loss as low as 1dB and crosstalk lower than -25 dB.

1 Introduction

Silicon photonics (SiP) has become established as leading integrated photonics technology [1]. It brings together high integration density while being compatible with the already established microelectronic CMOS process allowing mass production. Datacom is an important application area of SiP [2]. The data rate requirements for these optical links keep increasing as data intensive services become more popular. Wavelength Division Multiplexing (WDM) data links are used to achieve high aggregated data rates without increasing the symbol rates, which are limited by the modulator and demodulator bandwidths. Wavelength (de)multiplexer is one of the key components in WDM systems. Various WDM demultiplexing schemes have been proposed for the SiP platform including ring resonators filters, lattice-form filters, arrayed waveguide gratings (AWGs) and echelle gratings (EGs) [3].
The curved waveguide grating (CWG) demultiplexer was proposed by Hao et al. as a promising alternative to the conventional architectures [4] and it was demonstrated experimentally for the silicon-on-insulator (SOI) platform by Bock et al. [5]. Figure 1 shows a schematic of a CWG demultiplexer. It comprises a curved waveguide grating placed along a circle, a subwavelength grating (SWG) slab, a free propagation region (FPR) slab and output receiving waveguides positioned on the so-called Rowland circle. The SWG slab is a periodic structure that synthesizes an artificial metamaterial with a properly designed effective refractive index [6,7].

First experimental demonstrations of CWG demultiplexers exhibited high insertion losses (~4 dB) [5], which made this component un-attractive for practical applications. We recently showed that those losses were due to off-chip radiation as the diffraction induced by the waveguide grating was not entirely directed to the FPR slab and an important fraction was radiated upwards and downwards [8]. Here, we demonstrate for the first time a CWG demultiplexer that frustrates off-chip radiation by operating the grating waveguide in the single beam condition [9]. For doing so, we judiciously design de diffractive grating period and the lateral SWG slab metamaterial to frustrate phase-matching condition in the silica cladding region while allowing it in the SWG region. As a result, we demonstrate experimentally a demultiplexer that has both low loss (~ 1 dB) and low crosstalk (< -25 dB) in the SOI platform.

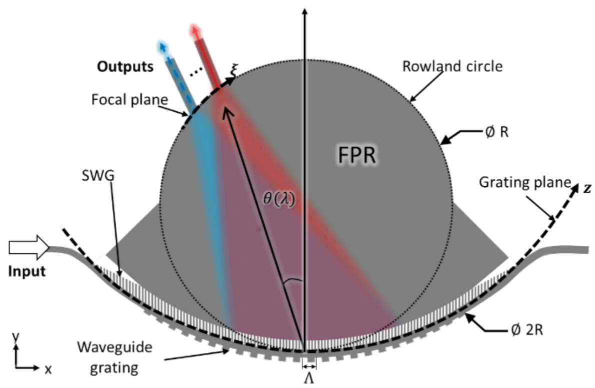

Fig. 1. Schematic of a curved waveguide grating demultiplexer. The blue and red coloured areas show the diffracted light focusing on different output waveguides for different wavelengths.

2 Fundamentals and design

The light entering the device from the input waveguide is progressively diffracted by the waveguide grating. The SWG region intercepts and conducts the diffracted light into the FPR. The light propagates through the FPR and is focused on the Rowland circle. To fulfil the single beam condition, output waveguides are placed at an angle $\theta \approx$

* Corresponding author: abdel@uma.es

−35° from the grating normal. This introduces aberrations in the image formation that needs to be corrected to achieve a sharp image. This is done by judiciously chirping the grating pitch. The demultiplexing functionality comes from the dispersive nature of the waveguide grating which makes diffraction angle θ to vary with wavelength. The diffraction angle is given by the grating equation:

$$\theta(\lambda) = \text{asin}((n_{FB} - \lambda/\Lambda)/n_S)$$

where, n_{FB} is the waveguide grating Floquet-Bloch mode effective index, λ is the free-space wavelength, Λ is the waveguide grating period and n_S is the effective index of the FPR slab. We investigate a demultiplexer with channel spacing of 10 nm and the central wavelength of 1550 nm for in-plane (TE) polarization. The geometry of output waveguides and grating circle were designed by well stablished procedures [5]. The output waveguides width and separation were selected to set the grating length and limit the inter-channel crosstalk, respectively. The grating radius was designed to enforce a channel separation of 10 nm. To minimize the insertion loss, the off-chip radiation needs to be suppressed [9] and the image formed at the focal plane needs to match the receiving waveguide mode profile. For this purpose, we apodized the deflector grating following the procedure outlined in ref. [8].

3 Experimental characterization

The device was fabricated in a standard SOI platform wafer using electron beam lithography patterning and reactive ion etching.

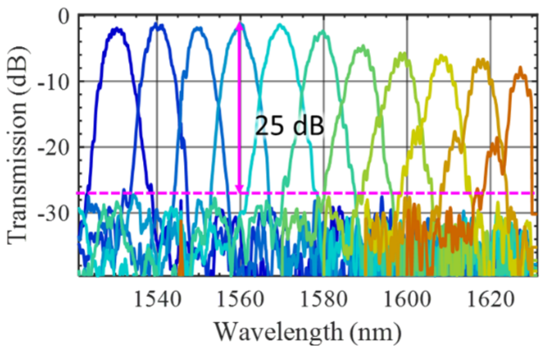

Fig. 2. Measured demultiplexer transmission spectra, from the input waveguide to the output waveguides.

The characterization was done by injecting a monochromatic, TE-polarized signal from a tunable laser source and measuring signal power at the output channels with a photodetector. An on-chip 3dB power splitter was used at the device input to extract a reference signal to determine the device transmittance. Figure 2 shows the measured transmission spectra for the device. We observe that channel separation and bandwidth closely match the designed ones. Central wavelengths of the output waveguides are shifted with respect to nominal values due to fabrication errors affecting the effective index of the grating waveguide. The best performing 6 output channels show insertion losses below 2 dB, with minimal loss below 1dB (channel 2) and the crosstalk is lower than -25 dB.

4 Conclusion

We have demonstrated an 11-channel, silicon photonic curved waveguide grating wavelength demultiplexer. We succeeded to dramatically reduce off-chip radiation by enforcing the single beam condition on the grating waveguide using metamaterial refractive index engineering.

Funding

Ministerio de Ciencia e Innovación (PID2019-106747RB-I00); Ministerio de Universidades (FPU16/03401); Junta de Andalucía (P18-RT-1453, P18-RT-793); FEDER Andalucía (UMA18-FEDERJA-219); Universidad de Málaga.

References

1. D. Thomson, A. Zilkie, J. E. Bowers, T. Komljenovic, G. T. Reed, L. Vivien, D. Marris-Morini, E. Cassan, L. Virot, J.-M. Fédéli, J.-M. Hartmann, J. H. Schmid, D.-X. Xu, F. Boeuf, P. O'Brien, G. Z. Mashanovich, and M. Nedeljkovic, J. Opt. **18**, 073003 (2016).
2. W. Shi, Y. Tian, and A. Gervais, Nanophotonics **9**, 4629 (2020).
3. K. Okamoto, IEEE J. Select. Topics Quantum Electron. **20**, 248 (2014).
4. Y. Hao, Y. Wu, J. Yang, X. Jiang, and M. Wang, Opt. Express **14**, 8630 (2006).
5. P. J. Bock, P. Cheben, J. H. Schmid, A. V. Velasco, A. Delâge, S. Janz, D.-X. Xu, J. Lapointe, T. J. Hall, and M. L. Calvo, Opt. Express **20**, 19882 (2012).
6. P. Cheben, R. Halir, J. H. Schmid, H. A. Atwater, and D. R. Smith, Nature **560**, 565 (2018).
7. R. Halir, A. Ortega-Monux, D. Benedikovic, G. Z. Mashanovich, J. G. Wanguemert-Perez, J. H. Schmid, I. Molina-Fernandez, and P. Cheben, Proc. IEEE **106**, 2144 (2018).
8. A. Hadij-ElHouati, P. Cheben, A. Ortega-Moñux, J. G. Wangüemert-Pérez, R. Halir, J. H. Schmid, and Í. Molina-Fernández, Opt. Express **27**, 33180 (2019).
9. A. Hadij-ElHouati, P. Cheben, A. Ortega-Moñux, J. G. Wangüemert-Pérez, R. Halir, J. de Oliva Rubio, J. H. Schmid, and I. Molina-Fernández, Opt. Lett. **46**, 2409 (2021).